Analysis of MDR1 P-Glycoprotein Conformational Changes in Permeabilized Cells Using Differential Immunoreactivity †

ARTICLE *in* BIOCHEMISTRY · MAY 2001

Impact Factor: 3.02 · DOI: 10.1021/bi001371v · Source: PubMed

3 AUTHORS, INCLUDING:

Todd E. Druley
Washington University in St. Louis
40 PUBLICATIONS **1,253** CITATIONS

Analysis of MDR1 P-Glycoprotein Conformational Changes in Permeabilized Cells Using Differential Immunoreactivity†

Todd E. Druley,‡ Wilfred D. Stein,§ and Igor B. Roninson*,‡

Department of Molecular Genetics, University of Illinois at Chicago, Chicago, Illinois 60607, and Department of Biological Chemistry, Hebrew University, Jerusalem, Israel 91904

Received June 15, 2000; Revised Manuscript Received November 7, 2000

ABSTRACT: The reactivity of the ATP-dependent multidrug transporter P-glycoprotein (Pgp) with the conformation-sensitive monoclonal antibody UIC2 is increased in the presence of Pgp transport substrates, ATP-depleting agents, or mutations that reduce the level of nucleotide binding by Pgp. We have investigated the effects of nucleotides and vinblastine, a Pgp transport substrate, on the UIC2 reactivity of Pgp in cells permeabilized by *Staphylococcus aureus* α-toxin. ATP, ADP, and nonhydrolyzable ATP analogues decreased the UIC2 reactivity; this effect was potentiated by vanadate, a nucleotide-trapping agent. The Hill number for the nucleotide-induced conformational transition was 2 for ATP and ADP but 1 for nonhydrolyzable ATP analogues. The Hill numbers for ATP and ADP were decreased to 1 by mutations in one of the two nucleotide binding sites of Pgp, whereas mutation of both sites greatly diminished the overall effect of nucleotides. Vinblastine reversed the decrease in the UIC2 reactivity brought about by all the nucleotides, including nonhydrolyzable analogues; this effect of vinblastine was blocked by vanadate. These data indicate that UIC2-detectable conformational changes of Pgp are driven by binding and debinding of nucleotides, that nucleotide hydrolysis affects the Hill number for its Pgp interactions, and that Pgp transport substrates promote nucleotide dissociation from Pgp. These findings are consistent with a conventional E1/E2 model that explains conformational transitions of a transporter protein through a series of linked equilibria.

Pgp[1] is a membrane transport protein and member of the ATP-binding cassette (ABC) transporter superfamily. It pumps many anticancer drugs out of tumor cells, causing one of the best-characterized forms of multidrug resistance in cancer (*1*−*3*). Pgp is expressed in many normal tissues and is a major component of the blood−brain barrier (*4*). Pgp encoded by the human *MDR*1 gene is a 170 kDa glycoprotein composed of two closely similar halves, each containing an ABC domain with a nucleotide-binding site (NBS) characterized by consensus Walker A and B sequence motifs, and a hydrophobic domain with six transmembrane segments (*5*). The hydrophobic domains of the protein appear to contain most of the sites that preferentially interact with its transport substrates (*1*, *6*). ATP is hydrolyzed as the protein pumps substrates, with a stoichiometry of 2 (or 2−3) ATP molecules consumed for each substrate molecule transported (*7*, *8*). ATP hydrolysis by Pgp was shown to be stimulated by its transport substrates (*9*). Despite this wealth of information, we do not yet fully understand how Pgp interacts with its transport substrates and nucleotides during its transport cycle.

Several groups have demonstrated that Pgp undergoes conformation changes during the process of pumping drugs out of the cell. Zhang and co-workers found that the tryptic digestion patterns of Pgp were altered by the presence or absence of nucleotides, phosphate and vanadate, suggesting that the protein existed in at least four different conformations according to which ligands are bound (*10*). Liu and Sharom labeled Pgp at the nucleotide-binding center with a fluorescent reporter group MIANS, whose emission is influenced by the hydrophobicity of its environment. Different conformations could be identified according to the ligands (nucleotides or drugs) bound to the protein (*11*). Also, by studying patterns of trypsin digestion, Julien and Gros have found that the presence of nucleotides alone or ATP with vanadate alters the tryptic digestion patterns of the murine Mdr3 Pgp (*12*). Sonveaux et al. (*13*) have studied the quenching of the intrinsic fluorescence of tryptophan residues within Pgp and shown that the level of quenching by a water-soluble reagent is increased markedly when nucleotides bind, and decreased when anthracycline drugs bind. Conformation changes have been studied in similar ways in many membrane transporters and have led to the development of detailed kinetic models for the action of these carriers and pumps (*14*). Similar detailed models for the action of Pgp (*15*−*17*) do not yet integrate the work on conformation changes.

† This work was supported by NIH Grant R37CA40333 (I.B.R.). W.D.S. was the recipient of a Yamagiwa-Yoshida Memorial International Cancer Study grant administered by the International Union Against Cancer (UICC).

* To whom correspondence should be addressed: Department of Molecular Genetics (MC 669), University of Illinois at Chicago, 900 South Ashland Ave., Chicago, IL 60607-7170. E-mail: roninson@uic.edu.

‡ University of Illinois at Chicago.

§ Hebrew University.

[1] Abbreviations: Pgp, P-glycoprotein; NBS, nucleotide-binding site; MIANS, 2-(4-maleimidoanilino)naphthalene-6-sulfonic acid; AMP-PNP, 5′-adenylylimidodiphosphate; ATPγS, adenosine 5′-*O*-(thiotriphosphate); 8-N_3ATP, 8-azidoadenosine 5′-triphosphate; FITC, fluorescein isothiocyanate; PBS, phosphate-buffered saline; BSA, bovine serum albumin; FACS, fluorescence-activated cell sorter; PI, propidium iodide.

10.1021/bi001371v CCC: $20.00
Published on Web 03/10/2001

We have undertaken a detailed investigation of the conformation changes that are revealed through the interaction between Pgp and a monoclonal antibody UIC2 (*18*, *19*). UIC2 blocks the action of Pgp as a functioning transporter when it binds to its epitopes from the external face of the cell membrane (*18*). The reactivity of UIC2 with intact cells is increased when Pgp drug substrates are present, when the cell's ATP levels are reduced by depletion, or when both nucleotide-binding sites of Pgp are mutated. These high- and low-reactivity states presumably reflect a conformational transition that the protein undergoes when it interacts with ligands (*19*). We reasoned that a full analysis of this system, which is unique in its ability to detect Pgp transitions in whole cells and in its native membrane environment, might reveal details of the pump's action. To this end, we have worked out a method which enables us to control the type and concentration of ligands that bind to Pgp, whether these are membrane permeable or impermeable. Experiments using this technique enabled us to demonstrate that UIC2-detectable conformational transitions of Pgp are driven by binding and debinding of nucleotides, that nucleotide hydrolysis affects the Hill number for its Pgp interactions, and that Pgp transport substrates promote nucleotide disassociation from Pgp. Our results suggest that the mechanism of Pgp function can be interpreted in terms of a conventional E1/E2 model of conformational transitions of a transporter protein.

EXPERIMENTAL PROCEDURES

Materials. ATP, ADP, AMP-PNP, ATPγS, 8-azido-ATP, AMP, CTP, UTP, ITP, GTP, $MgSO_4$, vinblastine, cyclosporin A, propidium iodide, and the ATP Bioluminescent Somatic Cell Assay Kit were from Sigma. *Staphylococcus aureus* α-toxin was purchased initially from Calbiochem and then from List Biological Labs. Sodium orthovanadate was from Fisher Scientific. The goat anti-mouse IgG2a fluorescein isothiocyanate (FITC)-conjugated antibody was obtained from Caltag Laboratories. The MRK16 monoclonal antibody was generously provided by T. Tsuruo (University of Tokyo, Tokyo, Japan). The isolation and preparation of the monoclonal antibody UIC2 have been previously described (*18*).

Cell Lines. LMtk$^-$ murine fibroblast cell lines, KK-H, KM-H, MK-H, and MM, were derived after transfection with either the wild-type (KK) or mutant (KM, MK, and MM) forms of human MDR1 cDNA (*20*) and were maintained in Dulbecco's modified Eagle's medium containing 10% fetal bovine serum, 1% glutamate, and a 1% penicillin/streptomycin mixture. Site-directed mutagenesis was used to generate the MK, KM, and MM mutants, which contain amino acid substitutions at either one (KM or MK) or both (MM) conserved lysine residues in the Walker A motifs of the N-terminal or C-terminal nucleotide-binding sites, K433M and K1076M, respectively.

The K562/i-S9 cell line was derived from human K562 leukemia cells by infection with a recombinant retrovirus carrying the human MDR1 cDNA followed by subcloning (without cytotoxic selection) and immunostaining for Pgp (*21*). K562/i-S9 cells were maintained in RPMI 1640 medium containing 10% fetal bovine serum, 1% glutamate, and a 1% penicillin/streptomycin mixture.

S. aureus α*-Toxin Permeabilization.* The concentration and time course of *S. aureus* α-toxin necessary to yield an approximate 50% distribution between permeabilized [propidium iodide (PI)-positive] and nonpermeabilized (PI-negative) staining cells were determined for each cell line in preliminary experiments. A concentration of α-toxin was chosen that was effective in 15−30 min at 37 °C. The approximate percentage of permeabilization was checked periodically under a light microscope via trypan blue staining and counting the percentage of blue cells per high power field. Permeabilization was performed in PBS and 1% BSA buffer at a final volume of 100 μL containing 1×10^6 cells at 37 °C. The reaction was stopped by the addition of 30 mL of 37 °C PBS, and the cells were centrifuged for 5 min at 1500 rpm at room temperature to wash away residual α-toxin and any substances released from the permeabilized cells. Following centrifugation, the supernatant was aspirated and the remaining cell pellet processed through the flow cytometry protocol described below.

Fluorescence-Activated Cell Sorting Assays. All primary antibody staining reactions were carried out in a final volume of 200 μL containing 1×10^6 cells/reaction mixture in phosphate-buffered saline (PBS) buffer with 1% bovine serum albumin (BSA). Cells were reacted with their respective nucleotides and/or drugs for 10−15 min at 37 °C prior to the addition of the primary antibody. UIC2 was aliquoted, heated at 48 °C for 24 h in a thermal cycler, and stored at 4 °C prior to use. It was determined that this treatment did not affect the reactivity of the antibody to Pgp in the presence of substrate, but decreased the reactivity of the antibody to Pgp in the absence of substrate (our unpublished data). Hence, the sensitivity of UIC2 for conformational transitions was increased. The concentration of the primary antibody that was used (15 μg/mL) had been previously determined as a saturating concentration of antibody for all available binding sites on 1×10^6 cells. Following addition of the primary antibody, the reaction mixture was held at 37 °C for an additional 30 min. Primary antibody reactions were stopped by the addition of 5 mL of ice-cold PBS buffer and the cells then centrifuged for 5 min at 4 °C and 1500 rpm. Pellets were resuspended in 100 μL of PBS and 1% BSA buffer containing 25 μg/mL goat anti-mouse FITC-conjugated secondary antibody. The reaction mixtures were left on ice (to prevent Pgp function) for 30 min before being stopped by the addition of 5 mL of ice-cold PBS buffer and centrifuged for 5 min at 4 °C and 1500 rpm. Immediately prior to analysis in the fluorescence-activated cell sorter (FACS), each pellet was resuspended in 350−500 μL of PBS and 1% BSA buffer containing 1 μg/mL PI. Two-color cytofluorometric analysis was performed by acquiring at least 10 000 individual events using a Becton Dickinson FacSort flow cytometer.

Flow cytometric data were analyzed by using the Becton Dickinson Information Systems CellQuest software. This analysis included cells contained in two specified regions, R1 and R2. The R1 region was defined by forward scatter, the measure of cell size, versus propidium iodide (PI) fluorescence, which distinguishes cells on the basis of their PI permeability. The R2 region was defined by forward scatter versus side scatter, the measure of cellular granularity. For all intact cell experiments, the R1 region was defined in such a way as to exclude all PI-positive cells and include only PI-negative cells.

For experiments in which permeabilized cells were studied, the R1 region was reset to include both PI-positive and PI-negative populations. The total number of acquired cells was increased to 25 000 to have a statistically significant number of gated events in both the PI-positive and PI-negative populations. For a given experiment, neither the size nor the granularity acquisition parameters were altered so as not to include artifactual events (e.g., membrane fragments) during the data analysis.

After acquisition had been completed, the FACS data were analyzed as follows. First, R1 and R2 regions that would be applied consistently to all reactions in a given experiment were defined. A single analysis (where the R1 region included only PI-negative cells) was performed for experiments in which intact cells were studied. Two separate analyses were performed for experiments in which α-toxin-treated cells were studied (one where the R1 region included only the PI-positive population and another where the R1 region included only the PI-negative population). For each reaction, all acquired cells falling within both R1 and R2 regions were displayed in a separate histogram and the statistics for each histogram, as determined by the CellQuest software, were calculated. These statistics included the median fluorescence (in arbitrary units) of the histogram population, which is the primary measurement of the UIC2 reactivity mentioned throughout these studies.

Data Analysis. We determined the kinetic parameters from the CellQuest-derived data using the SigmaPlot program. This gave us (1) the maximum or minimum fluorescence (F_{max} or F_{min}, respectively) at asymptotically high or low levels of vinblastine, nucleotide, or vanadate, (2) the concentration of vinblastine, nucleotide, or vanadate at which half of the maximal change in fluorescence occurs (K_m), and (3) the Hill number, *n*. The best-fit regression through the respective data points was determined using the appropriate binding isotherm, as follows. We used eq 1 for cases where the fluorescence signal, *F*, increases with *B*, the concentration of ligand, and eq 2 for those cases in which the fluorescence decreases, as stated in the text.

$$F = F_{min} + [(F_{max} - F_{min})B^n]/(K_m{}^n + B^n) \quad (1)$$

$$F = F_{min} + [(F_{max} - F_{min})K_m{}^n]/(K_m{}^n + B^n) \quad (2)$$

Bioluminescent Assay for ATP. Prior to ATP assessment, the cells were washed twice in room-temperature PBS by centrifugation at 1500 rpm for 5 min. Following washing and the aliquoting of 1000 cells per reaction, ATP-dependent luciferase bioluminescence was measured in a scintillation counter by using the protocol and reagents provided with the ATP Bioluminescent Somatic Cell Assay Kit.

Vanadate Treatment. Sodium orthovanadate was prepared fresh before each experiment by making a 100 mM stock solution and boiling the solution for 3 min prior to use. In intact cell experiments, 1×10^6 cells were incubated in PBS and 1% BSA buffer containing vanadate at a final volume of 100 μL for 1 h at 37 °C.[2] The reaction was stopped by the addition of 5 mL of ice-cold PBS and the mixture centrifuged at 1500 rpm for 5 min. In experiments involving α-toxin-treated cells, the cells were first treated with α-toxin, washed, and then reacted with vanadate in the presence of the appropriate nucleotide and an excess of $MgSO_4$ for 1 h at 37 °C before proceeding through the aforementioned FACS protocol.

[2] S. Dey, personal communication.

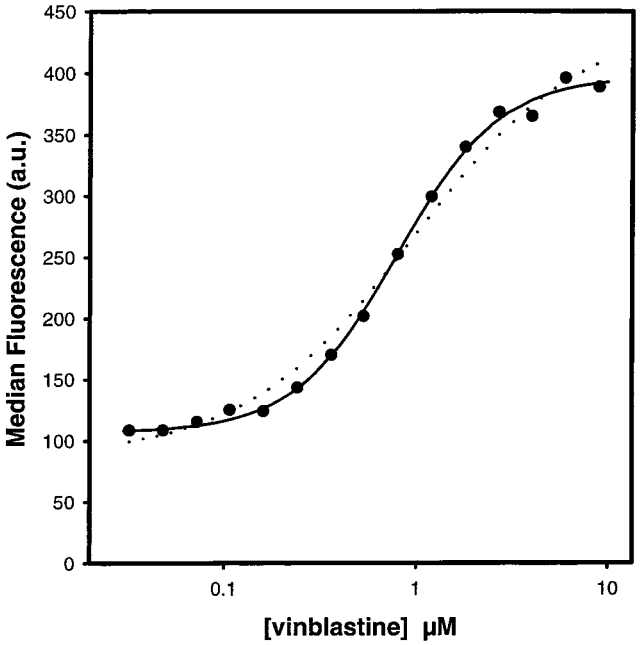

FIGURE 1: Effect of increasing concentrations of vinblastine on the fluorescence signal of intact K562/i-S9 cells stained with the UIC2 antibody. On the *X* axis is plotted the micromolar concentration of vinblastine. On the *Y* axis is plotted the median fluorescence of cells treated with UIC2 (arbitrary units). Cells were treated with vinblastine for 15 min at 37 °C prior to staining with UIC2 for 30 min at 37 °C: (●) median fluorescence. The solid line is the best-fit regression using eq 1 in Experimental Procedures, with a K_m of 0.79 ± 0.03 μM and an *n* of 1.64 ± 0.10. The dotted line is the best-fit regression with *n* held at 1.

RESULTS

Effects of Vinblastine and Vanadate on UIC2 Reactivity in Intact Cells. We have applied quantitative ligand-binding analysis to characterize interactions between Pgp and various drug and/or nucleotide ligands, which can be detected by altered UIC2 reactivity. As previously reported (*19*), UIC2 reactivity is increased by Pgp substrates, such as vinblastine, and ATP-depleting agents, such as sodium azide or oligomycin. These changes in antibody reactivity were interpreted to represent changes in Pgp conformation. In the study presented here, we have extended this analysis by using the same wild-type Pgp-expressing cell lines, K562/i-S9 and KK-H, that were used in the previous work (*19*). Figure 1 depicts the effect of increasing concentrations of vinblastine on the fluorescence of KK-H cells after indirect immunofluorescence staining with UIC2 at 37 °C. The fluorescence increases steadily with increasing concentrations of vinblastine. The solid line through the data points is the best fit using eq 1, a ligand binding isotherm with concentrations entering to the power *n*. The best-fit value for the K_m parameter, which represents the apparent affinity of the respective ligand for Pgp, was 0.79 ± 0.03 μM. The best-fit *n* value (the Hill number) was 1.64 ± 0.10, which is significantly greater than 1 at $p < 0.01$, as can also be seen by a comparison between the solid line and the dotted line,

which represents the best fit with n fixed at 1. The Hill number represents the *minimum* number of ligand molecules that are being bound in the reaction that is being studied. Thus, a Hill number of 1.64 is consistent with at least 2 molecules of vinblastine being required to bring about the conformation change from a low to a high UIC2 accessibility. This high Hill number and the value of K_m found in Figure 1 are both in excellent agreement with the results of other studies that measured the affinity and stoichiometry of vinblastine's interaction with Pgp (see the Discussion).

Our previous study suggested that the substrate-induced conformational transition of Pgp could be due to the stimulation of ATP hydrolysis or disassociation (*19*). This hypothesis predicts that irreversible nucleotide binding to Pgp should interfere with the substrate-induced increase in UIC2 reactivity. We have asked therefore if the effects of vinblastine on UIC2 reactivity would be affected by vanadate, an agent that inhibits the ATPase activity of Pgp in isolated membrane fractions (*22*) and in whole cells[2] by forming an irreversible ternary complex with ADP and Pgp (*22*). The effects of increasing concentrations of vanadate on the UIC2 reactivity of KK-H cells are shown in Figure 2A and for the K562/i-S9 cell line in Figure 2B. Cells were held in the presence of the indicated concentrations of vanadate for 1 h at 37 °C. Then, in the appropriate reaction mixtures, vinblastine was added and the mixture held for an additional 15 min at 37 °C prior to the addition of UIC2 and for an additional 30 min at 37 °C. Due to the slow rate at which vanadate crosses the intact plasma membrane, we reasoned that vanadate should be added and allowed to incubate prior to the addition of vinblastine. Cells stained with UIC2 in the absence of vinblastine (○) exhibit a slight decrease in UIC2 reactivity as the concentration of vanadate increases. In cells stained with UIC2 in the presence of vinblastine (●), vanadate strongly inhibits the ability of vinblastine to increase UIC2 reactivity, as predicted by our hypothesis. Vanadate exhibits maximal inhibition of the UIC2 reactivity at 4 mM in the K562/i-S9 cells and at 2 mM in the KK-H cells. Higher vanadate concentrations distorted the morphology of the KK-H cells to the extent that made FACS analysis impossible. Cellular reactivity toward MRK16, another Pgp-specific mAb, which reacts indifferently with the presence of ATP or drugs (*19*), was not affected in the presence of vanadate (△), indicating that vanadate does not alter the number of Pgp molecules on the cell surface.

Analysis of UIC2 Reactivity in Cells Permeabilized with the S. aureus α-Toxin. Up to this point, our studies have been carried out exclusively in intact cells. These studies could not definitively establish whether the UIC2-detectable conformational change was due to ATP hydrolysis or to the binding and debinding of nucleotide. To determine if nucleotide binding affects UIC2 reactivity, we needed to permeabilize the cells to nucleotides in a way that would preserve their morphology for FACS analysis. After some preliminary trials, we selected the *S. aureus* α-toxin as the permeabilizing agent. The *S. aureus* α-toxin forms a hydrophilic, aqueous pore within the plasma membrane, allowing the free passage of ions and molecules up to a molecular weight of 4000 (*23*). To identify permeabilized cells, we used propidium iodide (PI), which is commonly used in FACS assays as a marker for dead cells or other cells with a compromised plasma membrane. Figure 3A compares the

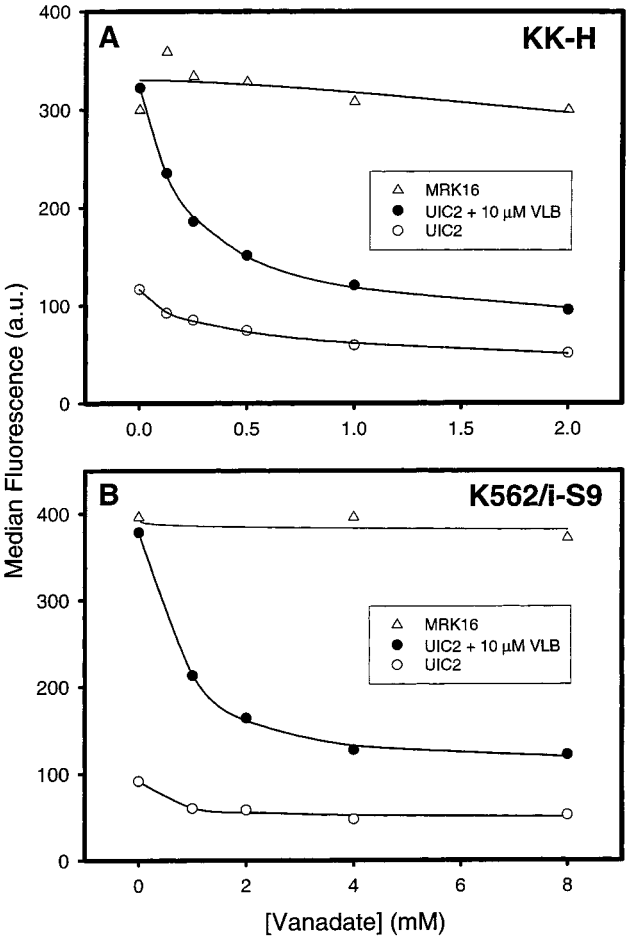

FIGURE 2: Effect of increasing concentrations of vanadate on UIC2 and MRK16 reactivity in intact KK-H (A) and K562/i-S9 (B) cells. Cells were pretreated for 1 h in different concentrations of vanadate and washed prior to the addition or omission of 10 μM vinblastine for 15 min at 37 °C followed by the addition of antibody for an additional 30 min at 37 °C. White circles (○) depict data for cells stained with UIC2 in the absence of vinblastine, and black circles (●) depict data for cells stained with UIC2 in the presence of vinblastine. White triangles (△) depict data for cells stained with MRK16 in the absence of vinblastine. In both panels, the solid line is the best-fit regression using eq 2 in Experimental Procedures.

PI staining and UIC2 reactivity of KK-H cells in three separate reaction mixtures under three different α-toxin treatment conditions. The top row of panels shows the fluorescence of cells that were not treated with α-toxin. The cells are negative for PI fluorescence and have a typical UIC2 reactivity profile. The middle panels show cells that had been treated with 25 μg/mL α-toxin (Calbiochem) at 37 °C for 30 min. PI staining reveals one population that is positive and one population that is negative for PI fluorescence, with both populations showing normal UIC2 reactivity profiles. As described in Experimental Procedures, each population can be analyzed individually to avoid artifacts introduced by the inclusion of other populations of cells or membrane fragments. The lower panels show cells that had been treated with 75 μg/mL α-toxin. These cells are almost entirely positive for PI fluorescence. However, the morphology of the cells was so damaged that no reliable UIC2 reactivity measurements could be ascertained with the FACS. On the basis of these results, we decided to use a regime of α-toxin treatments that yielded an approximate 50% distribution between PI-positive and PI-negative cells.

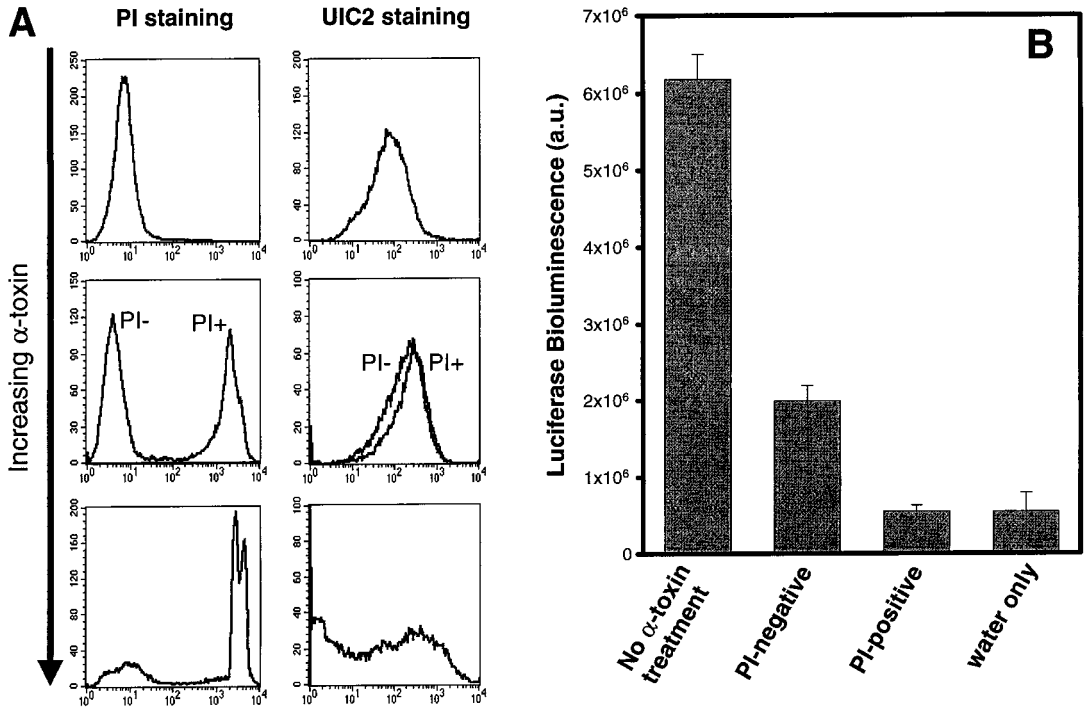

FIGURE 3: Effect of α-toxin permeabilization on fluorescence signals and intracellular ATP concentration. (A) Fluorescence profiles of KK-H cells stained with either PI (left column) or UIC2 (right column), pretreated for 30 min at 37 °C with increasing concentrations of the α-toxin: 0, 25, and 75 μg/mL (Calbiochem) from top to bottom. (B) K562/i-S9 cells were either pretreated with 50 μg/mL α-toxin (List Biologicals) for 15 min at 37 °C or untreated, stained with PI, and then sorted with a FACS. Following sorting, the intracellular ATP content of cells was measured using luciferase luminescence (see the text). Each column represents the mean of five separate determinations with bars indicating the standard error. The right-most column is the water-only blank.

We determined the extent of ATP depletion in the α-toxin-treated cells using a luciferase assay. Figure 3B shows the luciferase bioluminescence of K562/i-S9 cells that were held either in the presence or in the absence of an intermediate concentration of the α-toxin for 30 min at 37 °C, washed, and then sorted according to their PI fluorescence with the FACS. PI-positive cells exhibited the same amount of luciferase fluorescence as the background water blank, indicating nearly complete ATP depletion. In contrast, cells that had been treated with the α-toxin but remained PI-negative had a reduced, but far from zero, content of ATP. Permeabilization and washing thus eliminates the intracellular stores of ATP in PI-positive but leaves substantial amounts of ATP in PI-negative cells. (The difference in ATP content between the PI-positive α-toxin-treated cells and untreated cells is possibly due to the membranes of the PI-negative cell population being destabilized by α-toxin exposure. While these cells were sufficiently intact not to take in PI prior to FACS sorting, partial loss of ATP could have occurred during the FACS sorting and centrifugation prior to ATP analysis.) Apparently, the PI-negative cells in the α-toxin-treated samples maintained a sufficient amount of ATP for all the Pgp interactions, since these cells demonstrated levels of UIC2 reactivity that were essentially identical to those of untreated intact cells, in the presence of all the tested Pgp ligands (data not shown). The PI-negative population, therefore, provided an excellent internal control for the PI-positive cells, as both populations of α-toxin-treated cells were analyzed within the same reaction mixtures.

Effects of Nucleotides and Vinblastine on the UIC2 Reactivity of Permeabilized Cells. We compared the UIC2 reactivity of PI-positive cells stained in the presence of different nucleotides and in the presence or absence of a saturating concentration of vinblastine after α-toxin treatment. The results of these assays for KK-H cells are shown in Table 1; essentially the same results were obtained with K562/i-S9 cells (data not shown). The values in Table 1 are listed as the percent staining as compared to cells stained with UIC2 in the presence of 10 μM vinblastine alone, this giving the high level of UIC2 reactivity. Merely permeabilizing the cells and thereby removing intracellular ATP gave PI-positive cells a UIC2 reactivity that was comparable to the high level seen in the presence of vinblastine. The UIC2 reactivity of PI-positive (but not PI-negative) cells is significantly decreased in the presence of 4 mM ATP and its hydrolyzable analogue 8-N_3ATP, as well as ADP and the nonhydrolyzable ATP analogues AMP-PNP and ATPγS. In contrast, AMP, ITP, CTP, UTP, and GTP had little or no effect. Washing of the cells at 37 °C for 5 min reversed the nucleotide-induced decrease in UIC2 reactivity. The addition of 10 μM vinblastine after the nucleotide addition and prior to UIC2 staining also reversed the decrease in UIC2 reactivity that was induced by ATP, 8-N_3ATP, ADP, and the nonhydrolyzable ATP analogues. When the same assays were carried out in the presence of 1 mM vanadate, all the tested nucleotides at 2 mM (with a possible exception for AMP) produced a decrease in the UIC2 reactivity. In the presence of vanadate, the effect of the nucleotides was not reversed even by 20 μM vinblastine (Table 2). None of the manipulations described above altered cellular reactivity toward MRK16, indicating that these changes were specific for UIC2-detectable conformational transitions (Table 1 and data not shown).

Figure 4A depicts quantitative analysis of the effects of increasing ATP levels on the UIC2 reactivity of PI-positive K562/i-S9 cells. The solid line through the data points is

Table 1: Reactivity of α-Toxin-Treated KK-H Cells to UIC2 or MRK16 in the Presence or Absence of Nucleotides with or without Vinblastine[a]

	UIC2 PI-positive	MRK16 PI-positive	UIC2 PI-negative	MRK16 PI-negative
α-toxin only	87.5	95.6	25.3	96.3
VLB	100.0	100.0	100.0	100.0
ATP	38.2	92.2	21.3	90.4
ATP and VLB	101.8	90.6	94.7	97.2
ATP and wash	93.9	ND	27.6	ND
ADP	50.9	93.9	22.3	86.1
ADP and VLB	99.1	96.5	111.0	87.2
AMP-PNP	54.2	107.5	23.7	75.5
AMP-PNP and VLB	107.5	98.2	102.7	79.7
8-N_3ATP	33.7	ND	26.1	ND
8-N_3ATP and VLB	89.8	ND	112.4	ND
ATPγS	16.1	ND	12.8	ND
ATPγS and VLB	64.9	ND	93.1	ND

	UIC2 PI-positive	UIC2 PI-negative
α-toxin only	98.2	53.3
VLB	100.0	100.0
AMP	96.9	43.3
AMP and VLB	103.7	103.7
ITP	84.3	65.5
ITP and VLB	83.5	108.4
CTP	89.8	59.4
CTP and VLB	92.2	104.6
UTP	95.6	59.4
UTP and VLB	109.4	107.5
GTP	77.7	53.3
GTP and VLB	85.8	100.9

[a] KK-H cells were pretreated with 25 μg/mL α-toxin for 30 min at 37 °C and washed. At 4 mM, nucleotide was added or omitted for 15 min at 37 °C followed by the addition or omission of 10 μM vinblastine for 15 min and then antibody for an additional 30 min at 37 °C. Prior to FACS analysis, cells were stained with PI and antibody-associated fluorescence was analyzed separately for PI-positive and PI-negative cell populations. In each column, all values of the median fluorescence were normalized to that of vinblastine with no nucleotide set at 100. ND, not determined.

Table 2: UIC2 Reactivity of PI-Positive K562/i-S9 Cells in the Presence or Absence of 1 mM Vanadate with or without Nucleotide and/or Vinblastine[a]

	UIC2 staining, PI-positive cells
α-toxin only	95.6
VLB only	100.0
VAN only	93.9
VLB and VAN	108.4
ATP and VAN	37.2
ATP, VAN, and VLB	39.0
ADP and VAN	50.0
ADP, VAN, and VLB	41.4
AMP-PNP and VAN	67.9
AMP-PNP, VAN, and VLB	64.4
ATPγS and VAN	20.9
ATPγS, VAN, and VLB	20.9
8-N_3ATP and VAN	42.2
8-N_3ATP, VAN, and VLB	47.4
AMP and VAN	90.6
AMP, VAN, and VLB	79.1
GTP and VAN	53.8
GTP, VAN, and VLB	56.2
ITP and VAN	73.7
ITP, VAN, and VLB	71.7
CTP and VAN	58.8
CTP, VAN, and VLB	53.8
UTP and VAN	53.3
UTP, VAN, and VLB	56.7

[a] K562/i-S9 cells were first permeabilized as described in the Results. Cells were held in the absence or presence of vanadate with or without 2 mM nucleotide for 1 h at 37 °C. After 1 h, 20 μM vinblastine was added or omitted, and each reaction mixture was held for 15 min at 37 °C prior to the addition of UIC2 for an additional 30 min at 37 °C. Cells were stained with PI, and the UIC2-associated fluorescence of the PI-positive cell population was analyzed with a FACS. The median fluorescence values were normalized to that of vinblastine with no nucleotide set at 100.

the best-fit regression using eq 2 (Experimental Procedures), while the dotted line is the best fit with n fixed at 1. The K_m for the ATP-dependent decrease in UIC2 reactivity was 6.2 ± 0.8 mM, and the Hill number was 2.8 ± 0.8. The results of a similar experiment using ADP instead of ATP are shown in Figure 4B (●), where the K_m of the best-fit regression was 6.6 ± 0.5 mM and the Hill number was 2.2 ± 0.3, which was significantly different from 1. The addition of 2 mM vanadate decreased the K_m for ADP to 210 ± 30 μM [Figure 4B (○)]. The same effects were observed with KK-H cells (Figure 4C), where ADP produced a K_m of 4.7 ± 0.5 mM and a Hill number of 2.8 ± 0.8, but vanadate decreased the K_m to 140 μM. The presence of vanadate therefore increases the apparent affinity of ADP for Pgp by more than 30-fold, in agreement with the known nucleotide-trapping activity of vanadate.

Analysis of UIC2 Reactivity in P-Glycoprotein Nucleotide-Binding Domain Mutants. To determine whether the Hill numbers for ATP and ADP, which we found to be close to 2, reflect the binding of these nucleotides to the two nucleotide-binding sites of Pgp, we have used LMtk$^-$ transfectants carrying human Pgp with mutations in the Walker A motif of a single N-terminal (MK-H) or C-terminal (KM-H) NBS. In previous studies, these mutants have been shown to bind, but not hydrolyze, nucleotide (*20*) and to increase their UIC2 reactivity in the presence of Pgp substrates or ATP-depleting agents (*19*). As shown in Figure 5A, increasing concentrations of ADP decrease the UIC2 reactivity of the MK-H and KM-H cells. In contrast to cells expressing the wild-type Pgp, the Hill numbers for MK-H and KM-H cells were close to 1 (1.33 ± 0.19 and 1.04 ± 0.50, respectively). Similar experiments using either ATP or AMP-PNP instead of ADP also resulted in Hill numbers that were not significantly different from 1 (data not shown).

We have also analyzed the effects of nucleotides on the UIC2 reactivity of α-toxin-treated MM cells that express Pgp with mutations in both nucleotide-binding sites. These cells were shown to have a strongly decreased level of nucleotide binding and a high UIC2 reactivity, which was unaffected by drug substrates or ATP-depleting agents (*19*, *20*). In the absence of vanadate, the high UIC2 reactivity of PI-positive MM cells was almost unaffected by ADP [Figure 5B (○)] or by 4 mM ATP, AMP-PNP, or AMP (data not shown), as expected from mutations in both NBD domains of MM. In the presence of 1 mM vanadate, however, ADP significantly decreased the UIC2 reactivity of the MM cells with a K_m of 4 mM [Figure 5B (●)], and substantial decreases in UIC2 reactivity were obtained with all the tested nucleotides (5 mM), with the exception of AMP and CTP (data not shown). The largest decrease in UIC2 reactivity (as compared to that with vinblastine alone) was seen in the presence of vanadate with ATP (40.3%), ADP (47.0%), and ATPγS (43.3%).

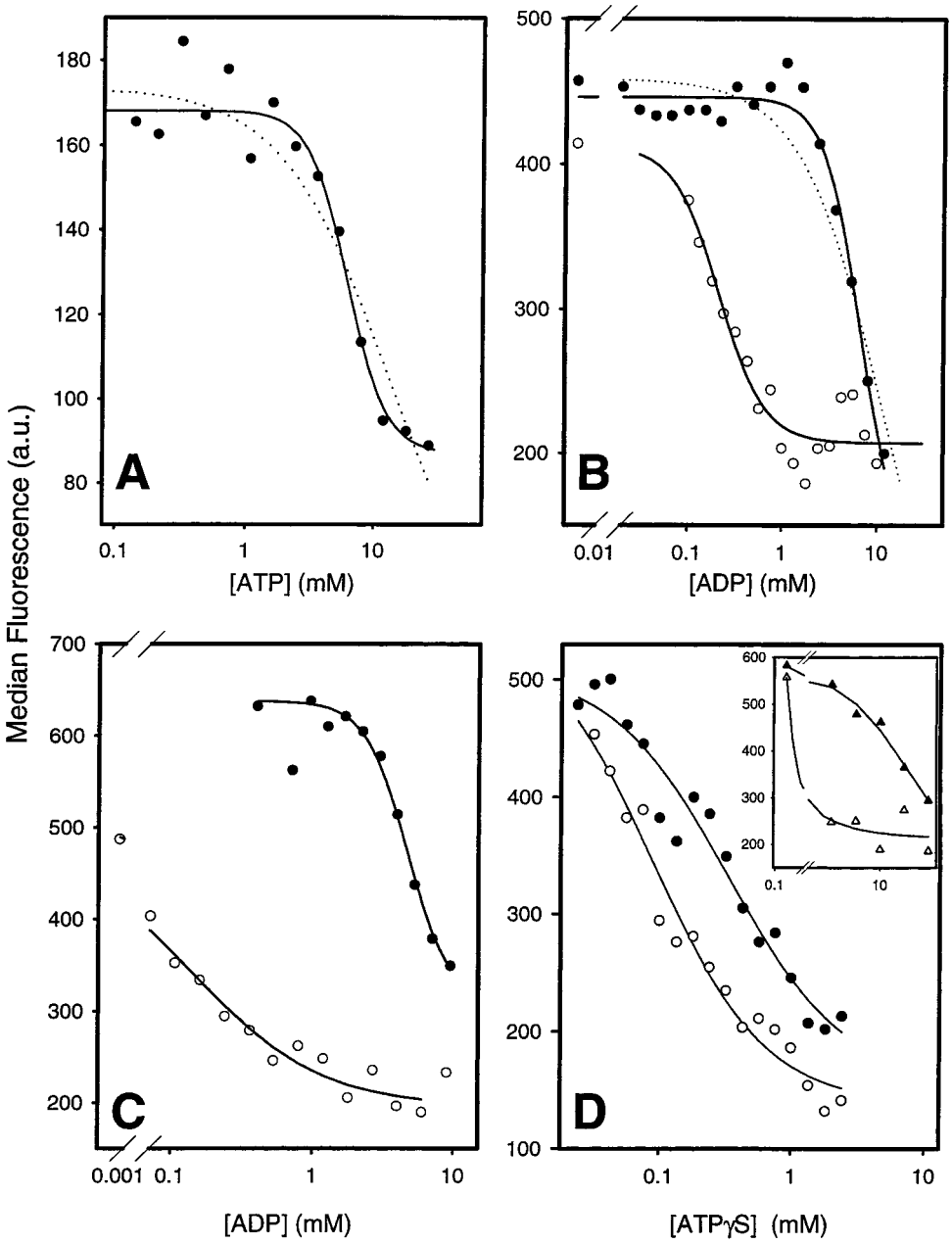

FIGURE 4: Effect of increasing nucleotide concentrations on the UIC2 reactivity in PI-positive K562/i-S9 (A, B, and D) and KK-H (C) cells. The median fluorescence of PI-positive cells stained in the absence (●) or in the presence (○) of vanadate was measured in the presence of increasing concentrations of ATP (A), ADP (B and C), or ATPγS (D). The inset in panel D shows the effects of ATPγS in the absence (△) or in the presence (▲) of 10 μM vinblastine. The solid line is the best-fit regression using eq 2 in Experimental Procedures, and the dotted line (A and B) is the best-fit regression with n held at 1. K562/i-S9 cells were treated with 50 μg/mL α-toxin for 15 min at 37 °C, and nucleotide with or without 2 mM vanadate was added for 1 h, followed by staining with UIC2 for an additional 30 min at 37 °C. KK-H cells were permeabilized with 1.5 μg/mL α-toxin for 20 min at 37 °C, and nucleotide with or without 1 mM vanadate was added for 1 h, followed by staining with UIC2 for an additional 30 min at 37 °C.

Effect of ATPγS on UIC2 Reactivity in the Presence of Vinblastine. The nonhydrolyzable ATP analogue ATPγS consistently provided the greatest decrease in UIC2 reactivity when compared to any other nucleotide, suggesting that it has the highest affinity for Pgp. Figure 4D demonstrates the effect of increasing concentrations of ATPγS in PI-positive K562/i-S9 cells (○). The best-fit regression lines, fit using eq 2, show that the K_m for ATPγS was 332 ± 111 μM. While not as dramatic as for ADP, vanadate improved the affinity of even this high-affinity nucleotide analogue by 3.7-fold (●). The Hill numbers for ATPγS, both in the presence and in the absence of vanadate, were 1.02 ± 0.13 and 0.96 ± 0.24, respectively. Another nonhydrolyzable ATP analogue, AMP-PNP, also gave a Hill number that was not significantly different from 1 (not shown), in striking contrast to ATP and ADP (which gave a Hill number close to 2).

As shown in Table 1, vinblastine reversed the decrease in UIC2 reactivity by all the tested nucleotides, whether hydrolyzable or not. The quantitative analysis of the effect of vinblastine on ATPγS is shown in the inset of Figure 4D, where white triangles (△) depict data for control cells (stained in the absence of vinblastine) while the black triangles (▲) depict data for cells stained in the presence of 10 μM vinblastine. The K_m for ATPγS in the absence of vinblastine was 0.31 mM compared to a K_m of 23 mM in its presence; i.e., vinblastine decreased the apparent Pgp affinity of

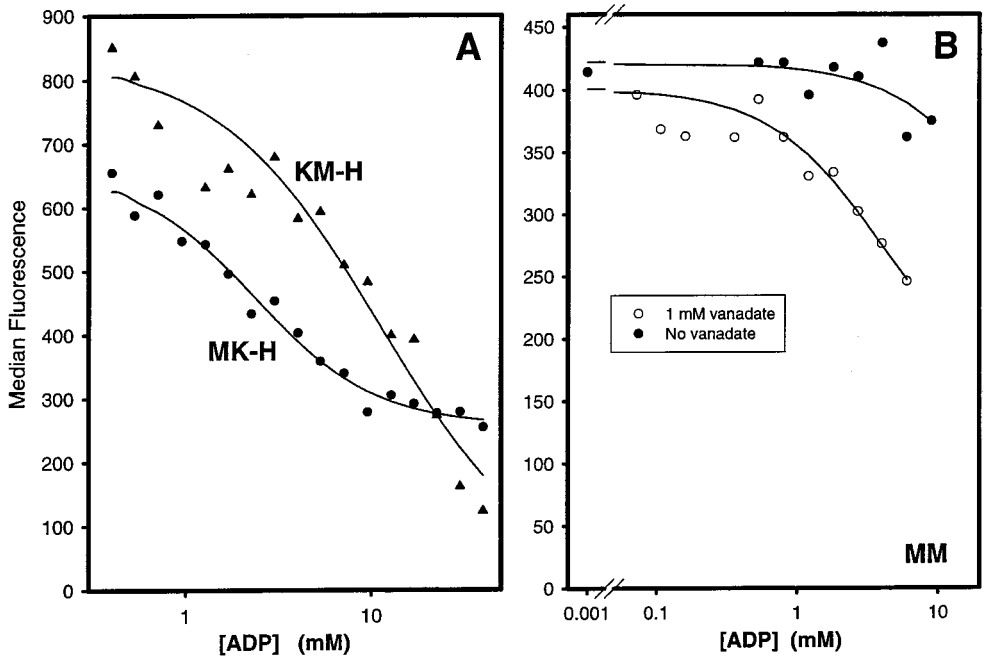

FIGURE 5: Effect of increasing concentrations of ADP on the UIC2 reactivity in PI-positive KM-H and MK-H (A) and MM cells (B). For each set of data, the solid line is the best-fit regression using eq 2 in Experimental Procedures. In panel A, KM-H (▲) and MK-H (●) cells were treated with 1.5 μg/mL α-toxin for 20 min at 37 °C. Thereafter, nucleotide was added for 15 min followed by staining with UIC2 for an additional 30 min at 37 °C. In panel B, MM cells were permeabilized with 1.5 μg/mL α-toxin for 20 min at 37 °C, and nucleotide with (○) or without (●) 1 mM vanadate was added for 1 h, followed by staining with UIC2 for an additional 30 min at 37 °C.

ATPγS, the strongest conformation-affecting nucleotide, by more than 60-fold. For all other nucleotides that decreased UIC2 reactivity, the reversal of their effect by vinblastine was even stronger than for ATPγS and too strong to accurately measure the K_m (data not shown).

DISCUSSION

Using the UIC2 reactivity shift as an assay for Pgp conformational transitions, we have investigated mechanistic aspects of the interactions between Pgp, nucleotides, and the Pgp transport substrate, vinblastine. We suggested in our previous study (*19*) that the change in mAb UIC2 reactivity of Pgp represents a conformational change in the protein. Indirect evidence suggested that this conformational change might be due to whether Pgp was bound to nucleotide. In the work presented here, we were able to prove this hypothesis, by developing a quantitative procedure for analyzing UIC2 reactivity changes in permeabilized cells. We have shown that the binding of nucleotide, irrespective of ATP hydrolysis, decreases UIC2 reactivity. Similarly, the ability of vinblastine to increase UIC2 reactivity also does not require nucleotide hydrolysis but can be explained by the stimulation of nucleotide debinding from Pgp, a previously unknown effect of Pgp transport substrates.

We have previously shown that Pgp transport substrates, ATP-depleting agents, or mutations of both Walker A motifs in the NBS of Pgp increase UIC2 reactivity (*19*). We have now demonstrated that nucleotide binding to Pgp produces the opposite effect, a decrease in UIC2 reactivity. We have shown this at first indirectly, by finding that vanadate, an agent that is known to trap nucleotides onto Pgp (*22*), decreases the UIC2 reactivity of intact cells (Figures 2 and 6). We have also demonstrated the effect of the nucleotides directly, by permeabilizing cells with the α-toxin and analyzing the UIC2 reactivity of the permeabilized cells in the presence or absence of different added nucleotides. α-Toxin permeabilization, which depletes the intracellular level of ATP, results in high UIC2 reactivity and is consistent with our previous findings for ATP depletion using metabolic

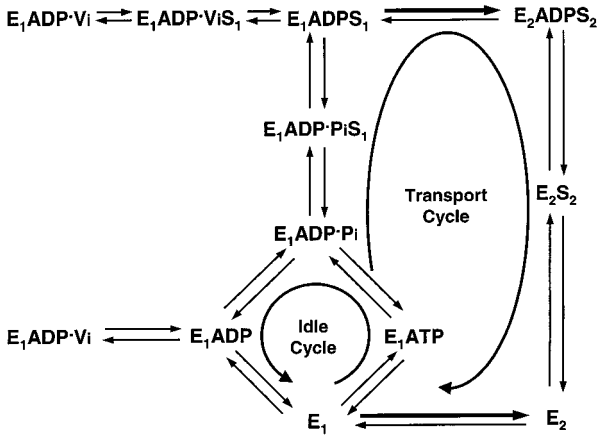

FIGURE 6: Proposed mechanism of Pgp function. E1 is defined as the state of the enzyme where the substrate-binding face of the protein is in an intracellular location. E2 is defined as the state of the enzyme where the substrate-binding face of the protein is in an extracellular location. In this model, E1 is equated with a low-UIC2 reactivity conformation of Pgp, while E2 is equated with a high-UIC2 reactivity conformation of Pgp. UIC2-detectable conformational transitions of Pgp occur during the E1ADPS1 to E2ADPS2 and E2 to E1 reactions. The presence of vanadate (V_i) traps Pgp in a highly stable ternary complex (*22*) that maintains a low UIC2 reactivity. In this scheme, the idle cycle refers to the basal level of ATP hydrolysis demonstrated by Pgp, while the binding of substrate (S) commits Pgp to the transport cycle that ultimately releases S on the extracellular surface of the plasma membrane.

inhibitors (*19*). The addition of either hydrolyzable or nonhydrolyzable nucleotides decreased UIC2 reactivity, indicating that ATP hydrolysis is not required for UIC2-detectable conformational transitions of Pgp.

The K_m for the decrease in UIC2 reactivity was high for both ATP and ADP, ~6 mM. This is nearly 1 order of magnitude higher than the K_m determined for the effect of ATP on the ATPase activity of Pgp (*24*, *25*) or for the effect of ADP on inhibiting this activity. Possibly, these high levels of added nucleotide are needed to offset the effects of endogenous ATPases. K_m values found for transport systems are complex functions of a number of linked chemical reactions (such as those shown in the model of Figure 6, which is described later in this section) and need not reflect the parameters of any particular step (*14*). The K_m, however, provides a measure of apparent affinity, which can be used as a relative parameter to evaluate the effects of different treatments.

The apparent affinity of nucleotide for Pgp was greatly increased by the simultaneous presence of vanadate, which has been previously shown to increase the apparent affinity of ATP and ADP by promoting nucleotide occlusion at Pgp (*22*). The presence of vanadate decreases the K_m more than 30-fold for ADP (Figure 4B,C) and nearly 4-fold for ATPγS (Figure 4D), which is consistent with a nucleotide-trapping activity of vanadate in our system. This interpretation is supported by the fact that only in the presence of vanadate did the MM mutant form of Pgp [which cannot hydrolyze but does, albeit poorly, bind ATP (*20*)] demonstrate a substantial decrease in UIC2 reactivity in the presence of ADP [Figure 5B (○)]. In addition to ATP and ADP, we have found that the effects of many nucleotides on UIC2 reactivity were potentiated by vanadate (Table 2), including nonhydrolyzable ATP analogues and non-adenine trinucleotides. These findings suggest that the stabilizing effect of vanadate on the binding of these ligands does not require their hydrolysis. This result was somewhat unexpected, since vanadate-mediated occlusion is usually viewed as the formation of a highly stable transition state analogue during ATP hydrolysis consisting of vanadate, Pgp, and ADP (*9*, *22*). Our results, however, are consistent with a report demonstrating that ADP can be trapped by vanadate without any ATP being present and that poorly hydrolyzable and nonhydrolyzable nucleotides also react with vanadate, inactivating the ATPase (*22*).

The Hill number describing the nucleotide-dependent decrease in UIC2 reactivity was determined to be significantly greater than 1 and close to 2 (Figure 4A−C), suggesting that pairs of ATP or ADP molecules are needed to decrease UIC2 reactivity. This result is consistent with the presence of 2 nucleotide-binding sites in each wild-type Pgp molecule and with our finding that the Hill number for ADP was decreased to 1 by mutations in either the N-terminal or C-terminal NBS (Figure 5A). The binding of 2 nucleotides to Pgp is also in agreement with the reports that 2 molecules of ATP are hydrolyzed for each substrate molecule that is transported (*1*, *7*) and that both ATP-binding sites must be intact if ATP hydrolysis (*20*, *24*), vanadate trapping (*17*, *26*), or drug efflux (*27*) is to occur.

In contrast to the case for ATP and ADP, a Hill number of 1, or not significantly different from 1, was determined for the effect of nonhydrolyzable ATP analogues (ATPγS and AMP-PNP) on UIC2 reactivity (Figure 4D). This surprising finding can be explained by the suggestion that a steric restriction exists that prevents 2 molecules of ATP or its analogues from being simultaneously bound to Pgp. However, no such restriction exists for 1 ADP and 1 ATP molecule or for 2 ADP molecules. The hypothesis that 2 ATP analogues cannot bind to Pgp at the same time is further corroborated by a paradoxical observation of Muller et al. (*20*). These authors showed that Pgps carrying mutations in either of the 2 Walker A motifs undergo photolabeling (which prevents nucleotide hydrolysis) with [^{32}P]-8-N_3ATP to the same maximal extent as wild-type Pgp. This finding can be interpreted by suggesting that the wild-type Pgp can bind only 1 molecule of [^{32}P]-8-N_3ATP, without hydrolysis. It has been previously suggested that the 2 ATP binding sites act in tandem so that ATP hydrolysis at 1 NBD is stimulated by ATP binding at the other NBD (*16*). Hence, the two-site binding that we observed for ATP can be interpreted as reflecting the coupled process of ATP hydrolysis at one site and binding at the other site, which cannot occur with the nonhydrolyzable analogues.

We have also used the UIC2 reactivity shift assay to characterize the interaction of Pgp with its transport substrate, vinblastine. The results of our quantitative analysis of the effect of vinblastine on UIC2 reactivity in intact cells showed good agreement with the conclusions of other investigators. The K_m determined for the vinblastine-dependent increase in UIC2 reactivity ($K_m = 0.79 \pm 0.03$ μM; Figure 1) is the same as the value of 0.77 ± 0.03 μM reported by Liu and Sharom (*11*) for the effect of vinblastine on quenching the fluorescence of the probe MIANS bound near the ATP-binding site of Pgp. It is also close to the K_m of 0.87 μM reported for the effect of vinblastine on competing with Pgp's pumping out of daunomycin (*3*, *28*, *29*). These apparent affinities of the nucleotide, observed in studies that measured Pgp conformation changes in the presence of nucleotide, either directly or as induced from transport events, are, however, far higher than the values found in direct binding assays in the absence of nucleotide (*30*−*32*), indicating that the K_m value for substrate binding is also a complex function, as discussed above for the apparent affinities of nucleotides.

The deduced Hill number for the effects of vinblastine suggests that the binding of 2 vinblastine molecules is required to trigger the conformation change from low- to high-level UIC2 binding. This conclusion is consistent with a number of similar findings. Thus, in the studies of Ayesh et al. (*33*), who measured the ability of vinblastine to block the Pgp-mediated transport of daunomycin, of Litman et al. (*29*) regarding the stimulation of the ATPase activity of Pgp by vinblastine, and of Shapiro and Ling (*8*) regarding the ability of vinblastine to block the efflux of both rhodamine and Hoechst 33342, which bind to different sites on Pgp, we find evidence for two sites for vinblastine. In the homologous LmrA ABC transporter from *Lactococcus lactis*, equilibrium binding studies of vinblastine also show clear evidence for two nonidentical sites on the pump for this drug (*34*). The authors find a clear stoichiometry of 2 drug molecules bound per molecule of transporter, which decreases to 1 in the presence of vanadate.

One of the most surprising results of this study is the finding that vinblastine is able to reverse the decrease in UIC2 reactivity induced in permeabilized cells by all the

tested nucleotides, whether hydrolyzable or not. Even with the nucleotide exhibiting the highest innate apparent affinity, ATPγS, vinblastine gave a 60-fold increase in the K_m (Figure 4D, inset), and this effect of vinblastine was even stronger with the other nucleotides. The ability of vinblastine to reverse the effect of nonhydrolyzable nucleotides can be explained by proposing that the Pgp transport substrates not only promote ATP hydrolysis by Pgp (*9*, *22*) but also stimulate nucleotide debinding from Pgp. This novel effect of Pgp transport substrates can also explain our finding that vinblastine can reverse the effects of ATP and ADP on the UIC2 reactivity of the KM and MK mutants, which have been shown (*20*) to be capable of nucleotide binding but not ATP hydrolysis.

It is informative to compare the results of this study with earlier studies of Pgp conformation changes. Liu and Sharom (*11*), using the fluorescence quenching of MIANS-labeled Pgp, found that ATP, as well as Pgp-transported drugs, reduced the fluorescence signal and that these changes were *additive* between the nucleotide and the transport substrates. In contrast, we find that the addition of nucleotides or drugs shifts the UIC2 fluorescence signal in *opposite* directions. Clearly, our probe (which binds to an extracellular epitope) and theirs (which is bound at the cytoplasmic face of the pump) are reporting on different regions of the Pgp molecule. The study by Sonveaux and colleagues (*13*) is very much complementary to ours. They studied the effect of a water-soluble quenching agent (acrylamide), present at the cytoplasmic face of Pgp embedded in vesicles, on the quenching of the intrinsic fluorescence of Pgp's tryptophan residues. These studies indicated that the nucleotides were forcing Pgp into a conformation in which most tryptophan residues were in a hydrophilic environment (susceptible to acrylamide quenching), whereas anthracycline substrates of Pgp had the opposite effect. The complementary nature of these two studies suggests that portions of the Pgp molecule could be *physically shifted* across the plane of the membrane, according to whether the nucleotide is bound or not bound. Such a shift is consistent with the results of Wang et al. (*10*), who showed that the patterns of proteolytic digestion of Pgp in membrane vesicles were altered by the addition of various nucleotides and vanadate. Interestingly, the list of nucleotides that altered the UIC2 reactivity in our study (Table 1) matches closely the list of nucleotides that were found by Wang et al. (*10*) and Julien and Gros (*12*) to alter the proteolytic patterns of Pgp. Thus, several independent types of analysis have produced consistent results regarding the conformational transitions that Pgp undergoes during its transport cycle.

To integrate the results of this study with other work analyzing various aspects of the mechanism of Pgp function, we propose the generalized scheme depicted in Figure 6. This scheme is based on the conventional two-conformation model that has proven to be very helpful in understanding transport events in a wide range of systems (*14*). Here, E1 and E2 are two conformations of the pump protein, where E1 has its drug (substrate) binding sites available at the cytoplasmic face of the membrane (side 1) and E2 has its drug binding sites accessible to the extracellular phase (side 2). S1 and S2 represent drug at sides 1 and 2 of the membrane, respectively. The "transport cycle" involves the binding of ATP to the pump, its hydrolysis to ADP and P_i, binding of the drug from side 1, a protein conformation change that allows the drug to access side 2, followed by debinding of the drug at side 2, and a conformation change to bring the drug-binding sites back to side 1. Figure 6 also includes the "idle cycle", a hydrolysis step not linked to drug movements and meant to account for the basal level of ATP hydrolysis in the absence of added drug. The idle cycle may conceivably be activated by the binding of the hypothesized "endogenous substrate". The scheme also shows interactions between vanadate (V_i) and the pump in the presence or absence of drug.

For simplicity, we have depicted a particular case in which nucleotide binds before drug, although a random order of binding is probably the truer situation. This highly simplified scheme also does not show that pairs rather than single molecules of ATP or drug interact with the pump during a transport cycle. Note that the two sites for vinblastine binding suggested by our data are not the S1 and S2 sites of Figure 6. In Figure 6, and in all similar schemes in the transport literature (*15*), states ES1 and ES2 interconvert and only one substrate molecule is bound to the transporter at any one time. For the glucose transporter of the human red blood cell, GLUT1, Carruthers and his colleagues (*35*) have shown that binding sites at both faces of the membrane can be present simultaneously, when the transporter exists as a homodimer. It is reasonable to speculate that Pgp may behave in a similar fashion.

The E1/E2 model of Figure 6 allows one to interpret the results of this study by hypothesizing that the E1 conformation of Pgp exhibits low UIC2 reactivity, whereas the E2 conformation has a high UIC2 reactivity. The finding that ATP-depleted cells in the absence of transport substrates demonstrate high UIC2 reactivity suggests that the equilibrium between free E1 and free E2 is in favor of E2 (i.e., E2 happens to be the form with a lower free energy). We further hypothesize that substrate-bound ES2 forms are more stable than ES1 forms. When a nucleotide is present, the E1 state predominates and the UIC2 signal is low. In contrast, binding of vinblastine shifts the system to the E2 state, resulting in a high UIC2 signal. All equilibria are assumed to be conventionally reversible. Therefore, the excess of drug, even in the presence of a bound nucleotide, will shift the system to an E2 state. The concentration of drug required to do so may well be far larger than would be required to bring about such a shift in the absence of nucleotide, or at low nucleotide concentrations. Similarly, stabilization of the E1 state in the presence of nucleotide would require high concentrations of vinblastine to bring about the shift to E2. Such shifting equilibria are conventionally invoked to account for the different apparent affinities that various ligands have for a pumping system (*14*). Binding of V_i has the effect of "pulling" the linked equilibrium between E1 and ADP away from E2 forms, thus increasing the apparent affinity of the nucleotide. Finally, we can explain the stimulation of nucleotide debinding by vinblastine by assuming that the loss of ADP or any other bound nucleotide from E2 occurs more readily than from E1. Further studies should verify the validity of the essential aspects of this proposed model.

ACKNOWLEDGMENT

We thank Dr. Takashi Tsuruo for the gift of the MRK16 antibody, Dr. Eugene Mechetner for providing some of the

UIC2 antibody, Drs. Svetlana Salov and Eugenia Broude for help with antibody preparations, and Adam Ruth and Dr. Saibal Dey for helpful discussions and suggestions.

REFERENCES

1. Ambudkar, S. V., Dey, S., Hrycyna, C. A., Ramachandra, M., Pastan, I., and Gottesman, M. M. (1999) *Annu. Rev. Pharmacol. Toxicol. 39*, 361−398.
2. Gottesman, M. M., and Pastan, I. (1993) *Annu. Rev. Biochem. 62*, 385−427.
3. Stein, W. D. (1997) *Physiol. Rev. 77*, 545−590.
4. Schinkel, A. H., Smit, J. J. M., van Tellingen, O., Beijnen, J. H., Wagenaar, E., van Deemter, L., Mol, C. A. A. M., van der Valk, M. A., Robanus-Maadag, E. C., te Riele, H. P. J., Berns, A. J. M., and Borst, P. (1994) *Cell 77*, 491−502.
5. Chen, C. J., Chin, J. E., Ueda, K., Clark, D. P., Pastan, I., Gottesman, M. M., and Roninson, I. B. (1986) *Cell 47*, 381−389.
6. Hafkemeyer, P., Dey, S., Ambudkar, S. V., Hrycyna, C. A., Pastan, I., and Gottesman, M. M. (1998) *Biochemistry 37*, 16400−16409.
7. Eytan, G. D., Regev, R., and Assaraf, Y. G. (1996) *J. Biol. Chem. 271*, 3172−3178.
8. Shapiro, A. B., and Ling, V. (1997) *Eur. J. Biochem. 250*, 130−137.
9. Sarkadi, B., Price, E. M., Boucher, R. C., Germann, U. A., and Scarborough, G. A. (1992) *J. Biol. Chem. 267*, 4854−4858.
10. Wang, G., Pincheira, R., Zhang, M., and Zhang, J. T. (1997) *Biochem. J. 328*, 897−904.
11. Liu, R., and Sharom, F. J. (1996) *Biochemistry 35*, 11865−11873.
12. Julien, M., and Gros, P. (2000) *Biochemistry 39*, 4559−4568.
13. Sonveaux, N., Vigano, C., Shapiro, A. B., Ling, V., and Ruysschaert, J. M. (1999) *J. Biol. Chem. 274*, 17649−17654.
14. Stein, W. D. (1986) *Transport and diffusion across cell membranes*, Academic Press, Orlando, FL.
15. Dey, S., Ramachandra, M., Pastan, I., Gottesman, M. M., and Ambudkar, S. V. (1997) *Proc. Natl. Acad. Sci. U.S.A. 94*, 10594−10599.
16. Senior, A. E., Al Shawi, M. K., and Urbatsch, I. L. (1995) *J. Bioenerg. Biomembr. 27*, 31−36.
17. Urbatsch, I. L., Beaudet, L., Carrier, I., and Gros, P. (1998) *Biochemistry 37*, 4592−4602.
18. Mechetner, E., and Roninson, I. (1992) *Proc. Natl. Acad. Sci. U.S.A. 89*, 5824−5828.
19. Mechetner, E. B., Schott, B., Morse, B. S., Stein, W. D., Druley, T., Davis, K. A., Tsuruo, T., and Roninson, I. B. (1997) *Proc. Natl. Acad. Sci. U.S.A. 94*, 12908−12913.
20. Muller, M., Bakos, E., Welker, E., Varadi, A., Germann, U. A., Gottesman, M. M., Morse, B. S., Roninson, I. B., and Sarkadi, B. (1996) *J. Biol. Chem. 271*, 1877−1883.
21. Chaudhary, P. M., and Roninson, I. B. (1991) *Cell 66*, 85−94.
22. Urbatsch, I. L., Sankaran, B., Weber, J., and Senior, A. E. (1995) *J. Biol. Chem. 270*, 19383−19390.
23. Bhakdi, S., and Tranum-Jensen, J. (1991) *Microbiol. Rev. 55*, 733−751.
24. Loo, T. W., and Clarke, D. M. (1995) *J. Biol. Chem. 270*, 21449−21452.
25. Ramachandra, M., Ambudkar, S. V., Chen, D., Hrycyna, C. A., Dey, S., Gottesman, M. M., and Pastan, I. (1998) *Biochemistry 37*, 5010−5019.
26. Szabo, K., Welker, E., Bakos, E., Muller, M., Roninson, I. B., Varadi, A., and Sarkadi, B. (1998) *J. Biol. Chem. 273*, 10132−10138.
27. Azzaria, M., Schurr, E., and Gros, P. (1989) *Mol. Cell. Biol. 9*, 5289−5297.
28. Shao, Y. M., Ayesh, S., and Stein, W. D. (1997) *Biochim. Biophys. Acta 1360*, 30−38.
29. Litman, T., Zeuthen, T., Skovsgaard, T., and Stein, W. D. (1997) *Biochim. Biophys. Acta 1361*, 169−176.
30. Callaghan, R., Berridge, G., Ferry, D. R., and Higgins, C. F. (1997) *Biochim. Biophys. Acta 1328*, 109−124.
31. Dale, I. L., Tuffley, W., Callaghan, R., Holmes, J. A., Martin, K., Luscombe, M., Mistry, P., Ryder, H., Stewart, A. J., Charlton, P., Twentyman, P. R., and Bevan, P. (1998) *Br. J. Cancer 78*, 885−892.
32. Martin, C., Berridge, G., Mistry, P., Higgins, C., Charlton, P., and Callaghan, R. (1999) *Br. J. Pharmacol. 128*, 403−411.
33. Ayesh, S., Shao, Y. M., and Stein, W. D. (1996) *Biochim. Biophys. Acta 1316*, 8−18.
34. van Veen, H. W., Margolles, A., Muller, M., Higgins, C. F., and Konings, W. N. (2000) *EMBO J. 19*, 2503−2514.
35. Sultzman, L. A., and Carruthers, A. (1999) *Biochemistry 38*, 6640−6650.

BI001371V